

Enhanced Optimization Strategies to Design an Underactuated Hand Exoskeleton

Baris Akbas¹, Huseyin Taner Yuksel¹, Aleyna Soylemez¹,
Mine Sarac², *Member, IEEE*, and Fabio Stroppa¹, *Member, IEEE*

Abstract—Exoskeletons can boost human strength and provide assistance to individuals with physical disabilities. However, ensuring safety and optimal performance in their design poses substantial challenges. This study presents the design process for an underactuated hand exoskeleton (U-HEX), first including a single objective (maximizing force transmission), then expanding into multi objective (also minimizing torque variance and actuator displacement). The optimization relies on a Genetic Algorithm, the Big Bang-Big Crunch Algorithm, and their versions for multi-objective optimization. Analyses revealed that using Big Bang-Big Crunch provides high and more consistent results in terms of optimality with lower convergence time. In addition, adding more objectives offers a variety of trade-off solutions to the designers, who might later set priorities for the objectives without repeating the process – at the cost of complicating the optimization algorithm and computational burden. These findings underline the importance of performing proper optimization while designing exoskeletons, as well as providing a significant improvement to this specific robotic design.

Index Terms—Prosthetics and Exoskeletons, Rehabilitation Robotics, Mechanism Design, Evolutionary Computation and Optimization.

I. INTRODUCTION

EXOSKELETONS are wearable robotic devices that can improve users' functional abilities during physically challenging tasks [1]–[3] or assist/rehabilitate them in case of functional disabilities [4]–[6]. They are usually designed to be worn on a specific body location; thus, their proper design is crucial for force transmission efficiency but also, and most importantly, for users' safety [7]. For an exoskeleton to be safe, designers must consider the alignment between the anatomic and mechanical joints and possible (intentional or unintentional) movements of users during operation [8], [9]. In addition, the exoskeleton design must be optimized to provide the highest level of well-distributed output forces through small and lightweight actuators.

The engineering design process is usually performed through mathematical optimization, which is the search for the best element (*optimum*) within a set of alternatives (decision variables' values) based on one or more specific criteria (*objectives*) [10]–[12]. Traditional optimization methods rely on numerical and calculus-based techniques [13] and might be challenging for solving exoskeleton design [14] due to



Fig. 1. The optimized device for the index finger component of U-HEX.

properties such as non-discrete domains, non-differentiability, multimodality, discontinuity [15], and the need for reliability [16] and robustness [17]. Alternatively, the nature-inspired Evolutionary Computation (EC) methods – particularly Evolutionary Algorithms (EAs) – are well-known and effective in dealing with engineering optimization problems [18] and often with exoskeleton design [14].

Previously, we proposed optimizing an underactuated hand exoskeleton (U-HEX [19], shown in Fig. 1) using EAs, in which we retrieved the best set of link lengths (decision variables) that maximize the output force transmission (objective function) [20]. While the first design of U-HEX was optimized with a naive-deterministic search approach, which iteratively analyzed each possible combination of design parameters (i.e., “brute force”), we employed a Genetic Algorithm (GA) [21], [22] and the Big Bang-Big Crunch algorithm (BBBC) [23]. Comparative analyses revealed that both EAs yielded more consistent and optimal solutions than brute force in a significantly shorter time. This allowed us to extend the search space by including more decision variables to the problem (i.e., three more link lengths in the design), significantly improving U-HEX's efficiency.

However, our previous work had a few limitations. Firstly, we only investigated the impact of different optimization methods over a single objective function. Secondly, although we included mechanical constraints to ensure the device's safety and operational efficiency, we did not constrain the desired actuator movements to reach a natural range of motion for the user's hand. In other words, we have found an *optimal*

This work is funded by TÜBİTAK project number 123M690 and partially funded by TÜBİTAK project number 121C145 and 121C147.

¹Computer Engineering, Kadir Has University, İstanbul, Turkey. E-mail: fabio.stroppa@khas.edu.tr

²Mechatronics Engineering, Kadir Has University, İstanbul, Turkey.

set of link lengths with no prior assumption on the desired actuator displacements. This assumption cannot be overlooked, since our design involves a linear actuator with a physical limit to how much it could move from its base. In fact, choosing the suitable actuator for an exoskeleton design is a challenging step involving many factors [24]. For the U-HEX design, a linear DC motor was selected due to its low cost and compact design – so that it can fit on top of the hand [19]. Therefore, it is crucial to minimize the desired range of actuator displacement to assist natural ranges of motion for the finger joints *without* sacrificing the force transmission performance. On the other hand, we have previously constrained the ratio between the actuated finger joints in our optimization problem, while in reality, it would be preferred to be as close to 1 for well-distributed and safe force transmission.

In this study, we have built up on our previous single-objective optimization problem (SOOP) [20] by improving U-HEX's design in two alternative design processes:

- 1) we redefined the SOOP with an additional constraint to the maximum linear actuator displacement in parallel to the actuator chosen for the original design [19], and we hypothesize that this would result in a lower overall transmission and potentially different trends between different optimization methods – even though we have very effective optimization methods in hand (H_1); and
- 2) we extended the SOOP to a multi-objective optimization problem (MOOP) by *also* optimizing the balance between the torques applied to each finger joint and minimizing the linear displacement needed by the actuator (i.e., turning constraints into objectives), and we hypothesize that treating constraints as further objectives would better accommodate the problem and lead to a trade-off set of different designs balancing the device's properties (H_2).

Our contributions involve (i) providing a set of optimized designs for a state-of-the-art exoskeleton that was originally optimized with inefficient methods [19], (ii) providing a walk-through for a robotic design process that can be used as a guideline by future and less experienced robotic designers, (iii) comparing different algorithms and strategies for MOOPs to determine which one is most suitable for our design problem, and (iv) introducing two novel EC methods (NS-BBBC and SP-BBBC) suitable for robotic optimization.

The rest of the work is organized as follows: Sec. III describes and discusses the first design process, which optimizes U-HEX only considering a single objective (i.e., maximize the force transmission); Sec. IV describes and discusses the second design process, which optimizes U-HEX by adding two more objectives (i.e., distribute the distribution of forces to the finger and minimize the linear actuator displacement); Sec. V discusses the differences in the retrieved designs and the impact of each optimization process; and Sec. VI summarizes the work and presents future ideas.

II. EXOSKELETON DESIGN OPTIMIZATION

A. U-HEX Kinematics

U-HEX is a hand exoskeleton designed for hand rehabilitation, whose kinematic structure was detailed in its original

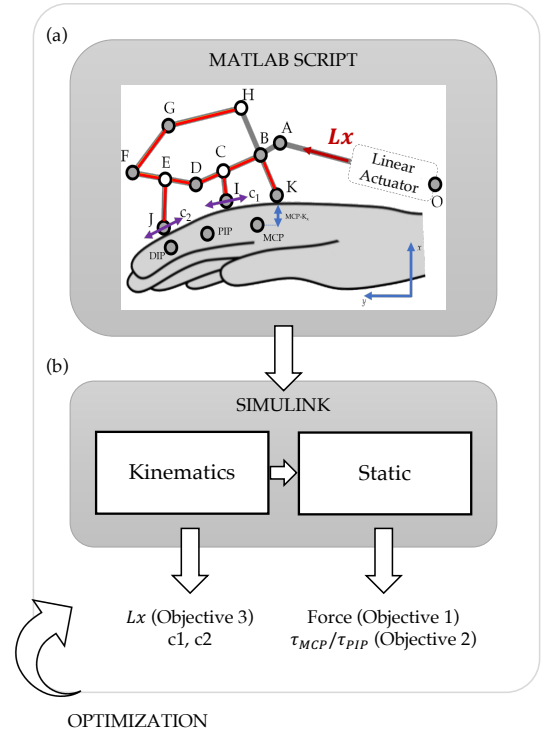


Fig. 2. Schematic of the optimization process for U-HEX: (a) its optimization problem; (b) its kinematics and statics to analyze its operation in terms of movements and force transmission. All the optimization algorithms are implemented in MATLAB. For a given set of link lengths, a Simulink model is executed to compute numerical inverse kinematics and analytical statics as the finger joints are iterated from fully open to fully closed.

work [19] and depicted in Fig. 2(a). Each gray dot represents a passive rotational joint (or anatomical finger joint) while empty circles (H , E , and C) are fixed points along rigid links with 90° fixed angle. The system has only one linear actuator between the points O and A . The exoskeleton is fixed on the hand from points K and O with variable lengths in the x and y directions. Finally, the exoskeleton is attached to the finger phalanges from points I and J with passive linear joint sliders represented as c_1 and c_2 , respectively.

B. Optimization Schema

U-HEX design is optimized to retrieve the optimal link lengths following the schema and design process summarized in Fig. 2. The decision variables of the problem are the link lengths (depicted as red lines in the figure). Specifically, the original design of U-HEX [19] was optimized considering only six link lengths: \overline{BC} , \overline{CD} , \overline{DE} , \overline{EF} , \overline{FG} , and \overline{GH} . This limitation was caused by the heavy computational requirements of brute force, which made it impossible to run the optimization with more link lengths. In our previous work [20], as well as in the current work, we included an additional three link lengths (\overline{BK} , \overline{CI} , and \overline{EJ}), potentially creating a more optimal solution. The bounds of the decision variables (i.e., the range of the link lengths) are reported in Table I and were chosen empirically in U-HEX's original work [19].

At each step of the process, a new set of link lengths is assigned by the optimization method in MATLAB. As shown

TABLE I
LINK LENGTH RANGES / DECISION VARIABLE BOUNDS

Main Six Link Lengths (mm)					
\overline{BC}	\overline{CD}	\overline{DE}	\overline{EF}	\overline{FG}	\overline{GH}
38 → 60	10 → 30	15 → 51	15 → 51	27 → 56	64 → 100
Additional Three Link Lengths (mm)					
\overline{BK}	\overline{CI}	\overline{EJ}			
20 → 50	10 → 17	20 → 50			

in Fig. 2 (b), this set is sent to a Simulink model (with a fixed-step solver) to compute the numerical inverse kinematics [19] as the finger joints are iterated from fully open (0°) to fully closed (80° for MCP and 90° for PIP). This process results in the corresponding movements around the passive joints (including the linear sliders c_1, c_2) and the desired actuator displacement (L_x). These movements are then used for the statics equations through analytical methods to compute the force transmission – i.e., expected torques around the finger joints (τ_{MCP}, τ_{PIP}) for a unit actuator force (1 N).

Obtaining the force transmission results terminates the Simulink file, while the MATLAB file evaluates the obtained performance in terms of the constraints and the optimality. Depending on the performance, the optimization algorithm repeats this loop until the requirements are satisfied.

C. Optimization Algorithms (Evolutionary Algorithms)

In this paper, we will explore two optimization problems (SOOP and MOOP) using the same optimization algorithms based on EC. EC is a sub-field of soft computing offering nature-inspired algorithms: instead of updating on a single point in the search space, it generates a population of potential solutions (i.e., a set of different combinations of decision variables' values) and evolves them toward the optimum using different metaheuristics (e.g., inspired by genetic recombination, natural selection, universe creation, animal behavior when foraging for food). Since the generic framework of EC methods does not rely on a specific mathematical model and can also tackle objective functions defined implicitly through simulations, they are particularly suitable for engineering problems such as optimizing the design of U-HEX. Specifically, we will employ two different EAs, as described below.

1) *Genetic Algorithm (GA)*: GAs are the most widely used EAs because they directly replicate the process of natural selection and the concept of survival of the fittest [22], [25]. As summarized in Algorithm 1, GA (i) creates a population of random solutions P within the problem's search space, (ii) assigns a fitness value to each solution based on the objective function, and (iii) produces new solutions Q by combining the values of the solutions in the current population through a process known as crossover. Only the fittest solutions M undergo crossover and are retained in subsequent generations, which allows the GA to evolve its population towards the problem's optimal solution. Similar to biological processes, the crossover operation utilizes the characteristics of high-quality solutions (parents) to generate new, comparable solutions (offspring), thereby accelerating convergence to an optimum. However, there is no guarantee that the retrieved optimum is global rather

than local. To address this issue, GAs incorporate an additional operator inspired by genetic mutation. This randomly alters the values of newly generated solutions, enhances search-space exploration, and helps in avoiding local optima.

Algorithm 1: Genetic Algorithm

input : Population size n , number of generations g
output: The most fitting solution $P(1)$

```

1 begin
2   P ← randomInitialization(n);
3   P ← evaluation(P);
4   for  $i \in [1, g]$  do
5     M ← selection(P);
6     Q ← variation(M);
7     Q ← evaluation(Q);
8     P ← survival(P, Q);
9   return P;
```

2) *Big Bang-Big Crunch Algorithm (BBBC)*: BBBC [23] is inspired by the universe's evolution through two phases: explosion and implosion. The process involves energy dissipation, which creates disorder and randomness, followed by the reorganization of this randomness into a new order. As summarized in Algorithm 2, BBBC (i) generates an initial random population P uniformly distributed across the search space (the explosion, or “big bang”), and (ii) evaluates and collects the population into their center of mass cm (the implosion, or “big crunch”). As the iterations progress, these two phases are repeated, with new solutions being generated closer to the center of mass, converging to the problem's optimal solution. BBBC is recognized for its superior convergence speed compared to GAs, making it a suitable choice for our problem, given the high runtime of the objective function caused by the execution of a Simulink simulation.

Algorithm 2: Big Bang-Big Crunch Algorithm

input : Population size n , number of generations g
output: The most fitting solution $P(1)$

```

1 begin
2   P ← randomInitialization(n);
3   for  $i \in [1, g]$  do
4     if  $i \neq 1$  then
5       P ← bang(cm, i);
6     P ← evaluation(P);
7     cm ← crunch(P);
8   return P;
```

III. DESIGN PROCESS I: SINGLE-OBJECTIVE OPTIMIZATION WITH MECHANICAL CONSTRAINTS

U-HEX was designed with a linear actuator (Firgelli L12-P) with a maximum displacement of 50 mm [19]. In this study, we evaluated the impact of presenting the mechanical limitations of the minimum and maximum linear actuator displacements on U-HEX design by comparing the optimality of their retrieved solutions against the original SOOP [20].

A. Optimization Problem (SOOP)

Similar to the previous work, the objective function is maximizing the force transmission during the operation:

$$\text{maximize } \sqrt{\tau_{MCP} + \tau_{PIP}} \quad (1)$$

where τ_{MCP} and τ_{PIP} are calculated based on the values of the decision variables (link lengths). The optimization problem is subject to the following seven inequality constraints (one constraint for each inequality):

- con_{1-4} : U-HEX is connected to the user's fingers through passive linear sliders (c_1 and c_2) whose movements should be limited by the user's finger size [19], resulting in four constraints defined in Eqn. (2) and (3);

$$0 \leq c_1 \leq 35 \quad (2)$$

$$0 \leq c_2 \leq 45 \quad (3)$$

- con_{5-6} : to guarantee a solid grasp and user's safety, the torques τ_{MCP} and τ_{PIP} should have a ratio within a reasonable range, resulting in two constraints defined in Eqn. (4) – this range comes from the static analysis from the original U-HEX work [19]; and

$$\frac{1}{15} \leq \frac{\tau_{MCP}}{\tau_{PIP}} \leq 15 \quad (4)$$

- con_7 : to ensure a natural range of motion for hand closing, the desired actuator displacement (L_x) must comply with the chosen actuator's mechanical spectrum, resulting in the constraint defined in Eqn. (5) – this constraint was not considered in our previous work [20].

$$L_x \leq 50 \quad (5)$$

Each of these constraints is a function of the decision variables (link lengths) and is calculated in Simulink, similarly to the objective function (see Fig. 2(a) [19]). Additional constraints to the problem are related to the decision variable bounds (i.e., the range of link lengths) reported in Table I.

B. Experiment Outline (SOOP)

To find the optimal design of U-HEX, we designed an experiment with three factors as (i) the constraint to the desired actuator displacement (with and without con_7), (ii) the optimization algorithm (GA and BBBC), and (iii) the number of decision variables (six and nine link lengths).

When the number of link lengths is limited to six, the additional three links are kept constant as $\overline{BK} = 37$, $\overline{CI} = 16$, and $\overline{EJ} = 37$. These values were selected empirically as detailed in the original work [19]. To ensure a valid comparison, we kept the algorithm parameters the same as our previous work [20], reported in Table II. Each algorithm was executed 10 times on a computer with 16 core 5.4 GHz CPU and 64 GB RAM.

C. Evaluation Metrics (SOOP)

At each execution, we recorded the set of optimized link lengths (i.e., values of the decision variables belonging to the most fitting solution in the population) and compared each factor in terms of two evaluation metrics.

TABLE II
PARAMETER SETTINGS IN SOOP FOR EAS
(DESIGN PROCESS I)

PARAMETER	EXPERIMENT VALUE
Max N. of Generations (GA, BBBC)	50
Population Size (GA, BBBC)	300
Selection Type (GA)	Binary Tournament [26]
Crossover Type (GA)	blx- α ($\alpha = 0.5$) [27]
Crossover Probability (GA)	1.0
Mutation Type (GA)	Polynomial [28]
Mutation Probability (GA)	0.2
Survival Strategy (GA)	Elitist ($\mu + \lambda$ schema) [29]
Crunch Method (BBBC)	Best Fit [30]
Constraint Handling (GA, BBBC)	Deb's Method [31]

1) *Optimality*: In SOOP, optimality is the value of the objective function, defined in Eqn. (1).

2) *Convergence Time (CT)*: CT indicates the time needed for algorithms to find the optimal solution, defined in Eqn (6).

$$CT = \frac{GC}{NG} \cdot RT \quad (6)$$

where the overall runtime (RT) indicates the overall time taken by the algorithm and the number of generations (NG) is 50 as indicated in Table II. The generation of convergence (GC) is the observed generation in which the algorithm converged to a solution – specifically if the variance in the value of the retrieved solution did not change in the last 20 iterations with a margin of 0.05 Nm.

D. Results (SOOP)

We analyzed optimality and convergence time using a three-way Repeated Measure Analysis of Variance (RM-ANOVA). Fig. 3 shows the mean and standard error of the collected data, as reported in Table III; whereas Table IV summarizes the ANOVA results.

1) *Results on Optimality*: Fig. 3 shows that adding the actuation constraint (con_7) to the optimization problem significantly lowered the force transmission. The drop between with and without con_7 becomes higher with nine decision variables compared to six. We further analyzed the trends between optimization strategies and decision variables *only* with con_7 through a post-hoc analysis, as depicted by a

TABLE III
NUMERICAL RESULTS OF DESIGN PROCESS I
WITH 6 AND 9 LINK LENGTHS (LL), WITH AND WITHOUT
ACTUATION DISPLACEMENT CONSTRAINT ($con_7: L_x \leq 50$)

	Force Transmission (Nm)	
	without con_7	with con_7
GA (6 LL)	31.63 \pm 0.01	28.39 \pm 0.10
BBBC (6 LL)	31.65 \pm 0.05	28.52 \pm 0.005
GA (9 LL)	56.20 \pm 0.41	28.61 \pm 0.19
BBBC (9 LL)	55.99 \pm 0.54	29.43 \pm 0.25
	Run Time (s)	
	without con_7	with con_7
GA (6 LL)	860.51 \pm 168.25	1857.05 \pm 32.84
BBBC (6 LL)	312.50 \pm 204.63	724.78 \pm 306.87
GA (9 LL)	1208.59 \pm 78.31	1772.48 \pm 182.43
BBBC (9 LL)	802.50 \pm 298.03	1391.63 \pm 469.05

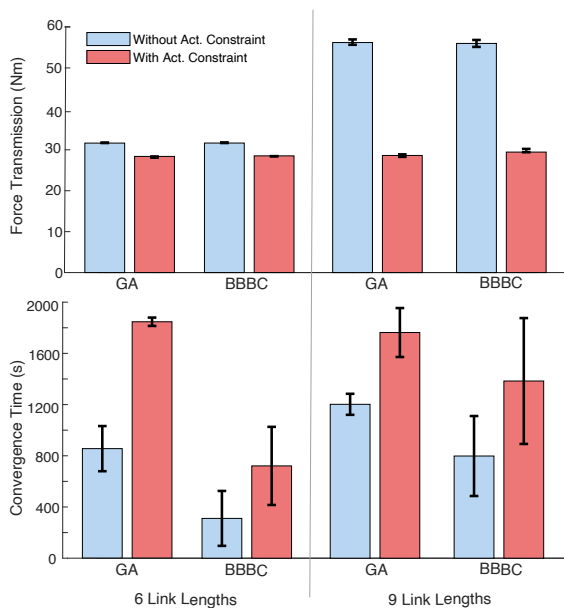


Fig. 3. Force transmission (optimality) and convergence time comparisons between experiments (with a different number of variable link lengths): with the constraint to the maximum actuator displacement ($con_7 = L_x \leq 50$) and without [20]. Plots report the mean and the standard error.

zoomed-in version in Fig. 4. We found that the optimality results are statistically significantly higher with nine decision variables ($F(1, 36) = 1047621.937, p < 0.001, \eta^2 = 1.000$) and while using BBBC ($F(1, 36) = 74.239, p < 0.001, \eta^2 = 0.673$). In addition, we observed their interactions to be statistically significant ($F(1, 36) = 38.156, p < 0.001, \eta^2 = 0.515$).

2) *Results on Convergence Time*: Fig. 3 shows that adding con_7 to the optimization problem significantly increased the convergence time for both EAs and the number of decision variables. We further analyzed the data collected with con_7 . We further analyzed the trends between optimization strategies and the number of link lengths *only* with con_7 through a post-hoc analysis. We found that the convergence time results are statistically significantly different with higher decision variables ($F(1, 36) = 9.001, p = 0.005, \eta^2 = 0.200$) and while using GA instead of BBBC ($F(1, 36) = 60.781, p < 0.001, \eta^2 = 0.628$). In addition, we found their interactions to be statistically significant ($F(1, 36) = 14.989, p < 0.001, \eta^2 = 0.294$).

E. Discussion (SOOP)

This experiment aimed to observe the impact of physical constraints on the optimization problem while using different EAs. We specifically added a constraint to the desired actuator displacement, which is given by the actuator chosen from the market (Firgelli L12-P), for a natural hand movement. We used two EAs (GA and BBBC) and compared our results to our previous study [20]. We hypothesized (H_1) that adding the additional constraint would lower the optimality (i.e., force transmission), regardless of the optimization technique. Our results in Fig. 3 show that including the actuation constraint lowers the force transmission while using both optimization methods and both decision variable settings (six and nine link lengths), as expected – therefore, H_1 holds true.

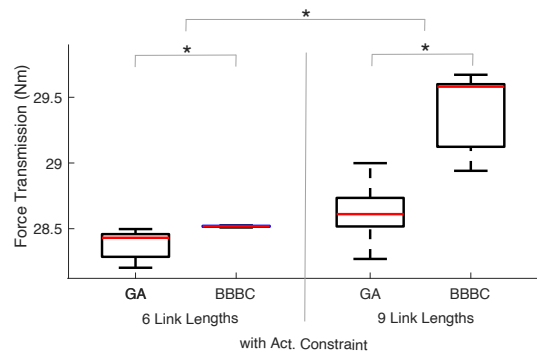


Fig. 4. A zoomed-in representation of force transmission (optimality) with the linear actuation constraint (con_7) as $L_x \leq 50$. The plots show the median, interquartile range, and outliers of the data.

Furthermore, Fig. 3 shows that increasing the number of decision variables from six to nine significantly increased the optimality without the actuation constraint, but not with it. This might indicate that all the solutions leading to high values of optimality require actuator displacements higher than 50 mm (i.e., unfeasible solutions), which will be investigated in the following design process with MOOP (see Sec. IV). In addition to a decrease in optimality, we observe that adding the actuation constraint resulted in statistically higher convergence times for the optimization algorithms. We speculate that higher convergence times might be due to the change in the search space and the computational toll of evaluating one more constraint, supported by the evidence in the literature [31].

We also analyzed the differences between the two EAs and the number of decision variables when the actuation constraint was implemented separately since the optimality results are primarily influenced by the optimization problem without the actuation constraint. Supported by further statistical analyses, Fig. 4 shows that increasing the number of decision variables provides a statistical increase in force transmission – similar to our previous study [20].

Interestingly, we observed that BBBC offers statistically higher optimality results than GA while working with six and nine decision variables independently – even though previously we found no difference between them [20]. We speculate that this was caused by the GA being stuck in a local maxima,

TABLE IV
STATISTICAL RESULTS FOR SOOP
IN TERMS OF OPTIMALITY AND CONVERGENCE TIME

	Optimality	Convergence Time
Algorithm (GA vs. BBBC)	$F(1,72)=9.351,$ $p=0.003, \eta^2 = 0.115$	$F(1,72)=45.624,$ $p<0.001, \eta^2 = 0.388$
N. of Link Lengths (6 vs. 9)	$F(1,72)=39221.829,$ $p<0.001, \eta^2 = 0.998$	$F(1,72)=7.992,$ $p=0.006, \eta^2 = 0.100$
Actuator Constraint (with vs. without)	$F(1,72)=57325.641,$ $p<0.001, \eta^2 = 0.999$	$F(1,72)=146.730,$ $p<0.001, \eta^2 = 0.671$
Algorithm \times N. of Link Lengths	$F(1,72)=3.209,$ $p=0.077, \eta^2 = 0.043$	$F(1,72)=0.722,$ $p=0.398, \eta^2 = 0.010$
Algorithm \times Constraint	$F(1,72)=21.140,$ $p<0.001, \eta^2 = 0.227$	$F(1,72)=0.164,$ $p=0.687, \eta^2 = 0.002$
N. of Link Lengths \times Constraint	$F(1,72)=35713.120,$ $p<0.001, \eta^2 = 0.998$	$F(1,72)=11.982,$ $p<0.001, \eta^2 = 0.143$
Algorithm \times N. of Link Lengths \times Constraint	$F(1,72)=13.668,$ $p<0.001, \eta^2 = 0.160$	$F(1,72)=0.046,$ $p=0.830, \eta^2 = 0.001$

which was significantly lower than the global maxima. This is also supported by observing the convergence time: while BBBC reached the current optimal solution¹ relatively fast, GA continued the search for a significantly longer time. This is also supported by the fact that the convergence time of GA did not change as much as BBBC when the number of decision variables was increased from six to nine. As mentioned in the state-of-the-art, BBBC was proposed to address some of the biggest disadvantages of GAs, such as premature convergence, convergence speed, and execution time [23].

IV. DESIGN PROCESS II: MULTI-OBJECTIVE OPTIMIZATION WITH MECHANICAL CONSTRAINTS

The design process in SOOP (Sec. III) showed the importance of considering the actuator displacement. Introducing a constraint to the desired actuator displacement (Eqn. 5) to perform natural hand movements reduced the force transmission of the exoskeleton but allowed it to be equipped with smaller actuators that can fit on top of the hand while still exerting a sufficient amount of force to assist users in opening and closing their fingers. In the meantime, users' safety was ensured by balancing the torques applied on both finger joints through two inequality constraints to bound the ratio between joint torques to be within a specific range as specified in Eqn. (4). Even though these constraints allowed us to have a design within safe and feasible boundaries, they do not ensure reaching an *optimal* one about these factors.

Based on these considerations, we re-defined the optimization problem to include two further objectives that were previously treated as constraints (i.e., con_{5-6} and con_7). We believe that turning constraints into additional objectives can help find better solutions by allowing more flexibility and balancing multiple requirements effectively, resulting in a set of different designs with different properties.

A. Background on Multi-Objective EAs (MOEAs)

MOOP involves optimizing two or more objectives simultaneously. These objectives usually conflict with each other (i.e., optimizing one might worsen the second, and so on), and it is not possible to retrieve a single solution that fully optimizes all the objectives simultaneously. Therefore, optimality in MOOP is defined by the concept of pairwise *dominance*: a solution x_1 dominates a solution x_2 if x_1 is not worse than x_2 in all objectives and x_1 is strictly better than x_2 in at least one objective [32]. When solutions do not dominate each other, then they are considered as optimal. This results in a set of trade-off solutions, each with different degrees of gain and losses to the objectives. This set is referred to as the *Pareto-Optimal Front*, or just Pareto Front.

EAs are great candidates for tackling MOOPs and looking for a set of solutions due to their population-based nature, allowing them to carry on different alternatives at a time [32]. These are usually referred to as Multi-Objectives Evolutionary Algorithms (MOEAs). MOEAs aim to retrieve an optimal

set (named the Pareto set) with the following properties: (i) convergence, or proximity to the true Pareto Front (which is unknown for engineering problems), and (ii) diversity, ensuring that the solutions are well-spaced so that the Pareto Front is uniformly covered. These properties are satisfied by different types of *Multi-Objective Survival Strategies* by removing weak solutions from the population. MOEAs usually generate a number of offspring larger than the set population size (useful to promote space exploration); however, this creates a surplus in the population. Survival strategies deal with this surplus by promoting non-dominated isolated solutions (*elites*) and removing the ones located in crowded regions to promote diversity. For this study, we will explore two of the most well-known strategies in the state-of-the-art.

a) *Non-Dominated Sorting with Crowding Distance (NS)*: Introduced with NSGA-II [33], NS (i) divides the population into different sorted non-dominated sets (i.e., the first set dominates all solutions, the second dominates all solutions except the ones in the first set, and so on); and (ii) deals with the surplus in the population with the crowding distance operator, which sums the normalized distances between neighboring solutions in each objective dimension it identifies isolated solutions (i.e., the larger the distance, the more isolated the solutions are).

b) *Strength Pareto Metric with Truncation (SP)*: Introduced with SPEA2 [34], SP (i) ranks each solution based on how many other solutions it dominates (strength); and (ii) deals with the surplus in the population with the truncation operator, which calculates the distance between for each solution and its k -th closest neighbor, removing the one with smallest distance (i.e., the smallest the distance, the more solutions are within that radius from the analyzed one).

We applied these two survival strategies to both EAs, resulting in four different MOEAs: the two based on GA are well-known state-of-the-art algorithms (NSGA-II [33] and SPEA2 [34]) whereas the two based on BBBC are new algorithms proposed in this work (NS-BBBC and SP-BBBC).

B. Optimization Problem (MOOP)

The MOOP is composed of three objectives:

- obj_1 : maximize the force transmission, the same objective optimized in Sec. III and expressed in Eqn. (1);
- obj_2 : balance the torques exerted on the two finger joints for well-distributed forces (i.e., minimize the torque variance), as expressed in Eqn. (7), which translates into minimizing the L1 norm distance between the torque ratio and 1; and

$$\text{minimize} \quad \begin{cases} \left| \frac{\tau_{MCP}}{\tau_{PIP}} - 1 \right| & \text{if } \tau_{MCP} \geq \tau_{PIP} \\ \left| \frac{\tau_{PIP}}{\tau_{MCP}} - 1 \right| & \text{otherwise} \end{cases} \quad (7)$$

- obj_3 : minimize the desired actuator displacement to assist a natural range of motion for the finger joints (L_x), as expressed in Eqn. (8).

$$\text{minimize} \quad L_x \quad (8)$$

¹We remind readers that EC methods retrieve approximate optimal solutions rather than the exact one.

The problem is subject to the same first four constraints defined in Sec. III-A for SOOP, except for con_{5-6} and con_7 that have been turned into obj_2 and obj_3 , respectively. Although these constraints allowed us to keep the torque variance within a safe boundary and the actuator displacement to be limited, they did not ensure that the torques were perfectly balanced and that the actuator displacement was minimized such that smaller actuators could be fit on the top of the device. Furthermore, we removed con_7 to allow the values of obj_3 to be unrestricted because we wanted to observe the values of obj_1 and obj_2 with a hypothetical longer actuator and map their boundaries – although these solutions will be unfeasible according to our actuation limits.

Additional constraints to the problem are related to the decision variable bounds (i.e., the range of link lengths), reported in Table I. Since our findings with SOOP showed that using nine decision variables results in better optimality, we used only nine decision variables for the MOOP.

TABLE V
PARAMETER SETTINGS IN MOOP FOR MOEAS
(DESIGN PROCESS II)

PARAMETER	EXPERIMENT VALUE
Max N. of Generations (GA, BBBC)	100
Population Size (GA, BBBC)	300
Selection Type (GA)	Binary Tournament [26]
Crossover Type (GA)	blx- α ($\alpha = 0.5$) [27]
Crossover Probability (GA)	1.0
Mutation Type (GA)	Polynomial [28]
Mutation Probability (GA)	0.2
Survival Strategy (GA, BBBC)	NS [33], SP [34]
Crunch Method (BBBC)	Best Fit [30]
Constraint Handling (GA, BBBC)	Constrained Tournament [32]

C. Experiment Outline (MOOP)

To find the optimal design of U-HEX, we designed an experiment with two factors as (i) the optimization algorithm (GA and BBBC) and (ii) the elitist multi-objective survival strategy (NS and SP). We investigate the impact of different algorithms and selection techniques. The algorithm parameters are reported in Table V, and retain the same values of Table II for the operation shared between SOOP and MOOP (e.g., crossover, mutation, bang, crunch). We increased the maximum number of generations from 50 to 100 because multi-objective algorithms tend to converge slower compared to single-objective counterparts due to the increased complexity of optimizing multiple conflicting objectives and the additional computational effort required to maintain a diverse set of solutions and evaluate Pareto dominance [33]. Each algorithm was executed 10 times on a computer with 16 core 5.4 GHz CPU and 64 GB RAM.

D. Evaluation Metrics (MOOP)

At each execution, we recorded the set of optimized link lengths (i.e., values of the decision variables belonging to the most fitting non-dominated set) and compared different runs with different factors in terms of two evaluation metrics.

1) *Optimality*: The optimality of MOOPs is based on two factors: (i) how close the solutions are to the Pareto front (convergence); and (ii) how diverse they are from each other in the objective space (diversity), such that the Pareto front is uniformly discovered. We evaluated these factors with the *hypervolume indicator* [35], a well-known metric measuring the volume of the objective space covered by a set of solutions normalized over the objectives (therefore, unitless). For problems with more than two objectives is subject to approximation, and it is not an exact geometrical value [36], [37]. Still, the hypervolume summarizes the convergence to the Pareto Front and the diversity of the solutions in the retrieved set in a single value: the larger the value, the better the algorithm performed (in the range $[0,1]$). Note that the hypervolume calculation for problems having more than two objectives is subject to approximation, and it is not an exact value [36], [37].

2) *Convergence Time (CT)*: Convergence time is calculated as in Eqn. (6) similar to SOOP (Sec. III-A), except GC is calculated on the hypervolume on a margin of $1.0E-4$.

E. Results (MOOP)

Each algorithm was executed 10 times, leading to 300 solutions. In total, out of the $(4 \cdot 10 \cdot 300 =)$ 12000 solutions, we found 3665 non-dominated solutions representing different trade-off exoskeleton designs – the excluded 8335 dominated solutions are worse than some of the non-dominated solutions in all the objectives. Fig. 5 shows the set of 3665 non-dominated solutions, in which every point of the plot represents the value in objective space (three dimensions) of a different combination of link lengths in the decision variable space (nine dimensions).

For each MOEA (specifically, each EA and survival strategy combination, see Sec. IV-C), we analyzed optimality and convergence time using a two-way RM-ANOVA. Fig. 6 shows the mean and standard error of the collected data, whereas Table VI reports the numerical results.

1) *Results on Optimality*: We first analyzed the retrieved solutions in terms of their objective function values. As shown in Fig. 5(c), there is a consistent and linear relationship between the objective functions related to the force transmission (obj_1) and to the actuator displacement (obj_3), making the Pareto front *almost* lie on a plane. Specifically, we observe that minimizing the actuator displacement results in lower force transmission while maximizing the force transmission requires larger amounts of actuator displacements – in line with what we found in the SOOP design (Sec. III-D). We quantified the strength of this linear relationship with the `corrcoef` function from Matlab (with 1 being the maximum strength), which yielded a coefficient of 0.976, indicating a high correlation between obj_1 and obj_3 . However, we did not observe any correlation between the other two objective functions (i.e., force transmission and torque variance or actuator displacement and torque variance).

Our two-way ANOVA results (Table VII) indicate that the optimality obtained by GA is not significantly different than BBBC. Yet, SP was found to be significantly better than NS

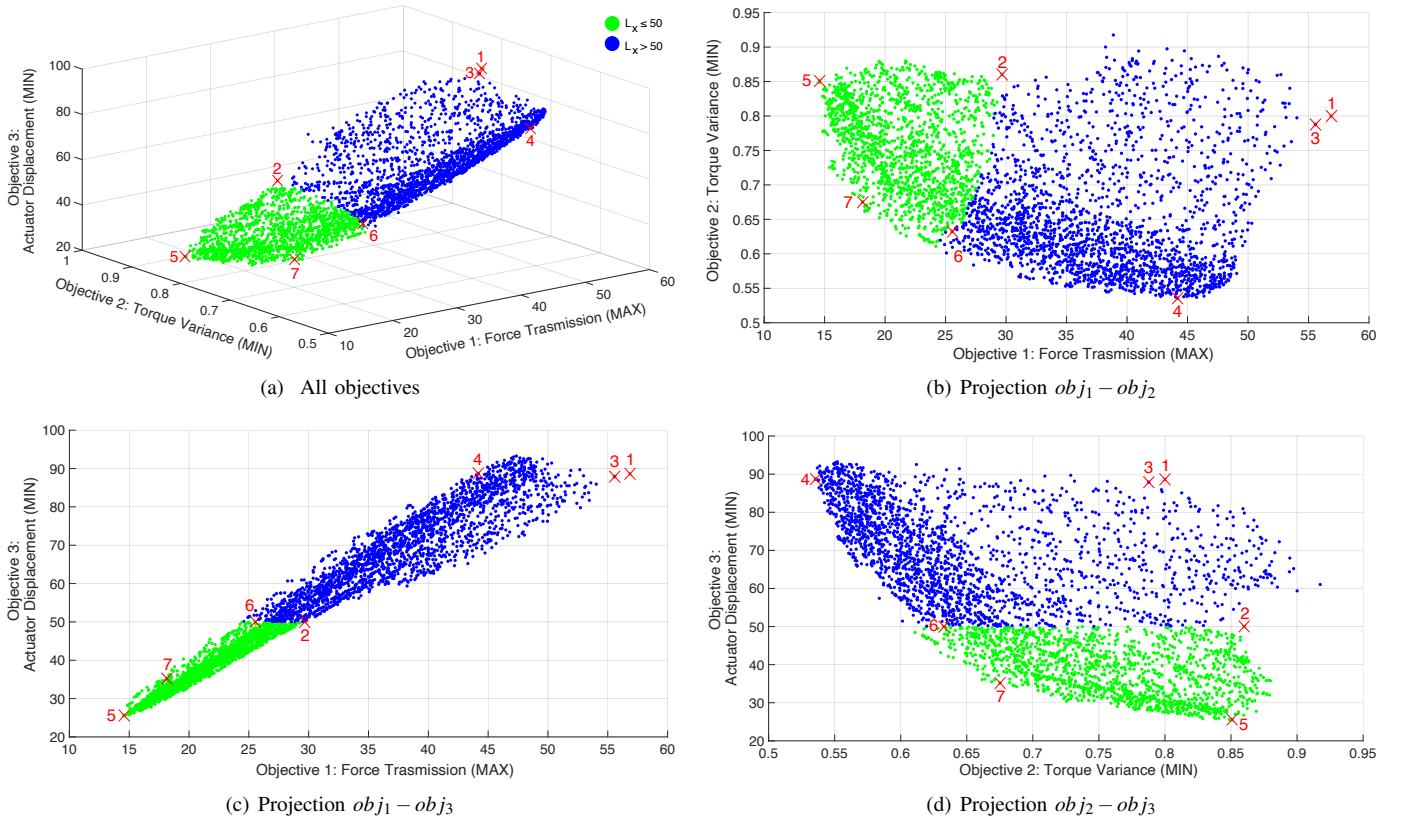


Fig. 5. All the non-dominated solutions (i.e., designs) retrieved by the four algorithms, collecting 3665 trade-off designs – designs having $L_x \leq 50$ are highlighted in green. In addition to Design 1 and 2 from the SOOP (reported in the figure but not belonging to this set), we selected five of designs (3-7) based on our preferences (numerical values are reported in Table VIII). Projection (c) shows a linear relation between force transmission and actuator displacement: longer actuators allow for higher force transmission.

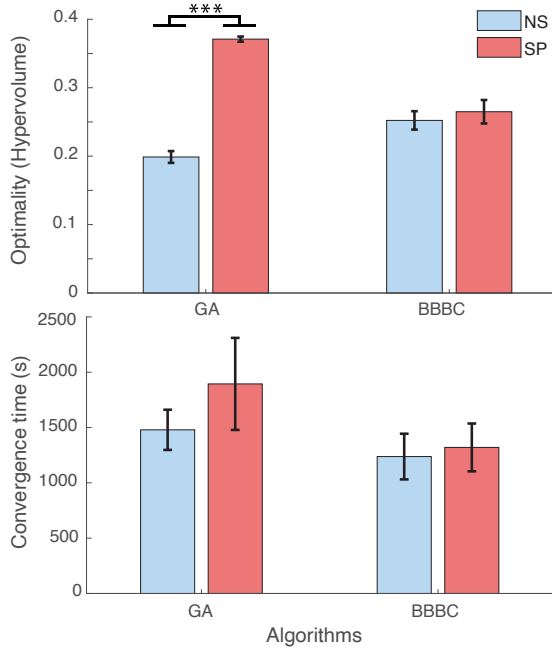


Fig. 6. Hypervolume indicator (optimality) and convergence time comparisons between MOOP experiments. Plots report the mean and the standard error.

in terms of optimality as it covered a wider area of the Pareto Front (see Table VI). We also observed that the interactions

Hypervolume Indicator		
	NS	SP
GA	0.19 ± 0.02	0.37 ± 0.01
BBBC	0.25 ± 0.04	0.26 ± 0.05
Run Time (s)		
	NS	SP
GA	1479.35 ± 574.48	1894.50 ± 1315.70
BBBC	1237.75 ± 652.51	1320.43 ± 683.40

to be significantly different than each other: NS was found to be more effective when used for BBBC compared to GA while SP was found to be more effective when used for GA compared to BBBC. In addition, we observe that choosing the survival strategy critically changed the optimality while using GA ($p < 0.001$) while it did not create such a drastic difference while using BBBC compared to using GA.

2) *Results on Convergence Time:* Fig. 6 and Table VI show the convergence time results obtained for all algorithms categorized as EAs and survival strategies. The results reported in Table VII indicate that there is no statistical difference between EAs, survival strategies, or their interaction.

TABLE VII
STATISTICAL RESULTS FOR MOOP, FOR THE MAIN FACTORS OF OPTIMIZATION ALGORITHM AND SURVIVAL STRATEGY, AND THEIR INTERACTION IN TERMS OF OPTIMALITY AND CONVERGENCE TIME

	Optimality	Convergence Time
Algorithm (GA vs. BBBC)	F(1,36)=3.159, p=0.109, $\eta^2=0.260$	F(1,36)=2.25, p=0.1421, $\eta^2=0.059$
Survival Strategy (NS vs SP)	F(1,36)=62.742, p<0.001, $\eta^2=0.875$	F(1,36)=0.84, p=0.3658, $\eta^2=0.023$
Algorithm \times Survival Strategy	F(1,36)=51.338, p<0.001, $\eta^2=0.851$	F(1,36)=0.37, p=0.5446, $\eta^2=0.010$

F. Discussion (MOOP)

This experiment aimed to observe the impact of optimizing multiple objective functions simultaneously while using four different MOEAs. MOEAs' efficiency in retrieving optima depends on survival strategies, which promote diversity by emphasizing non-dominated isolated solutions and removing the ones located in crowded regions. We tested two strategies (NG and SP), and we applied them to two EAs (GA and BBBC). We re-defined the SOOP by *also* minimizing the torque variance and the desired actuator displacement – which were introduced as constraints in the previous SOOP design process (see Sec. III).

Our optimality results with MOOP showed no significant difference between using different EAs (see Fig. 6 and Table VII). Interestingly, this is the same trend we observed for SOOP without con_7 [20] but not for SOOP with con_7 . Previously in Sec. III-E, we reported that BBBC showed significantly better optimality when con_7 is active and speculated that it might be caused by GA getting stuck in a local optimum, which was significantly worse than the global. The results of MOOP might be used as a support to our previous speculation since unconstraining the actuator displacement yielded similar trends to the results of SOOP without con_7 – even though we have a more complex optimization problem at hand.

On the other hand, our optimality results with MOOP showed that changing the survival strategy significantly changes the optimality – more importantly, depending on which EA is being used. Overall, using SP as a survival strategy is significantly better than NS. Observing the interactions between these trends brings more interesting outcomes: when applied to GA, NS was observed to be statistically significantly better than SP, which is in line with the literature stating that SPEA2 provides more optimal and diverse solutions at the expense of computational time [38]. However, we did not observe the same statistical difference with BBBC – although the set retrieved by SP-BBBC features a more uniform distribution than the one retrieved by NS-BBBC.

In light of these trends, we conclude that even though BBBC performs not statistically differently than GA, it yields more consistent results while changing conditions in the optimization problem (e.g., adding constraints and/or using another survival strategy). We can conclude that both optimization methods are valuable for different audiences: designers with a strong background in optimization (who might need many different conditions) could obtain a much better set of solutions with GA at the cost of more intense preliminary work. On the

other hand, designers who are unfamiliar with optimization might obtain more consistent results using BBBC.

The results also show that designers should be mindful of the objective functions before performing the experiment. Fig. 5(c) shows force transmission and desired actuator displacement are inversely proportional, which is also quantitatively supported by a high correlation coefficient. Increasing the actuator displacement results in higher force transmission. Considering that our motivation is to maximize the transmission while minimizing the displacement, satisfying them both would be an impossible task – a perfect example of conflicting objectives. Instead, designers might choose to treat one of these objectives as a constraint to avoid observing unfeasible solutions and to reduce the computational burden. On the other hand, this trend is mostly observable for solutions with $L_x \leq 50$ (obj_3); for longer actuators, the linearity starts deforming, as a non-convex region can be observed around 35 Nm of force transmission. If the actuator allows for those displacements, then having both objectives in the MOOP might be useful to explore alternative solutions – at the cost of increased weight for the exoskeleton, which must support a bigger and possibly more cumbersome actuator.

Lastly, we hypothesized that treating constraints as further objectives would better accommodate the problem and lead to a trade-off set of different designs balancing the device's properties (H_2). This approach offered distinct advantages by aiming to find solutions closest to a theoretical *ideal* point, where each objective achieves its optimal value. The set depicted in Fig. 5, which is a combination of solutions retrieved by four MOEAs over 40 runs, is a comprehensive evaluation of trade-offs featuring optimal solutions that are not constrained by predefined preferences. Ultimately, this allowed us to trace the shape of the objective space for U-HEX, understand the relationships between the objectives, and identify regions of interest. Therefore, H_2 holds true.

V. COMPARISON OF OPTIMIZED ROBOTIC DESIGNS

The optimization process provided us with two designs from SOOP (with $L_x \leq 50$ and with $L_x > 50$, respectively) and 3665 designs from MOOP – when considering nine link lengths as decision variables. Among these 3665 trade-off designs (i.e., equally optimal), we selected five of them based on our preferences. The numerical values of these seven designs are reported in Table VIII and graphically crossed on the objective space in Fig. 5 – including 1 and 2 from SOOP for comparison. Additionally, we drew the CAD models for designs having $L_x \leq 50$ mm to comply with U-Hex's linear actuator (Frigelli L12-P), depicted in Fig. 7. Design 1 and 2 were retrieved by BBBC, and they are the best solutions considering only force transmission as objective, whereas the MOOP designs were chosen based on the following criteria: Design 3 features the maximum force transmission (by SPEA2), Design 4 features the minimum in torque variance (by SPEA2), Design 5 features the minimum actuator displacement (by NS-BBBC), Design 6 features the maximum force transmission with an actuator displacement $L_x \leq 50$ (by SPEA2), and Design 7 features a good trade-off that balances all objectives (i.e.,

TABLE VIII
LINK LENGTHS AND OBJECTIVE VALUES OF THE SELECTED BEST DESIGNS (9 LINK LENGTHS)
BOLD OBJECTIVE VALUES INDICATE DESIGN SELECTION CRITERIA

RED OBJ3 VALUES INDICATE UNFEASIBLE SOLUTIONS DUE TO ACTUATOR DISPLACEMENT LONGER THAN 50 MM

	obj_1	obj_2	obj_3	\overline{BC}	\overline{BK}	\overline{EF}	\overline{DE}	\overline{CD}	\overline{EJ}	\overline{LLX}	\overline{CI}	\overline{AB}	\overline{KH}	\overline{GH}	\overline{GF}
Design 1 (SOOP)	56.86	0.80	88.60	60.00	48.50	51.00	15.00	10.00	36.54	20.00	10.98	20.00	72.00	91.37	56.00
Design 2 (SOOP)	29.67	0.86	50.00	57.09	40.30	15.00	15.00	10.00	42.72	20.00	16.00	20.00	72.00	100.00	56.00
Design 3 (MOOP)	55.57	0.79	87.88	60.00	47.78	50.87	15.05	10.13	36.07	20.00	10.00	20.00	72.00	91.73	56.00
Design 4 (MOOP)	44.18	0.54	88.70	59.54	46.65	50.54	15.01	16.81	50.00	20.00	10.29	20.00	72.00	98.15	56.00
Design 5 (MOOP)	14.58	0.85	25.57	38.07	20.00	15.99	29.51	12.65	39.84	20.00	10.37	20.00	72.00	92.46	31.36
Design 6 (MOOP)	25.55	0.63	49.99	46.59	26.30	51.00	21.25	12.51	50.00	20.00	10.83	20.00	72.00	88.97	55.97
Design 7 (MOOP)	18.15	0.68	35.22	38.00	20.00	44.84	34.81	11.14	48.95	20.00	10.96	20.00	72.00	94.62	55.43

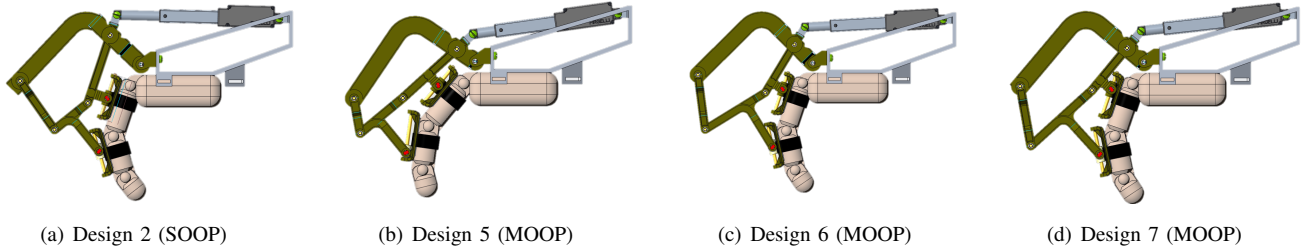


Fig. 7. CAD models of the designs retrieved by the optimization process, chosen among designs having $L_x \leq 50$ to comply with U-HEX’s linear actuator (Firgelli L12-P). Specifically, (a) the design from the SOOP along with three designs from the MOOP: with reference to Fig. 5, (b) Design 5 with minimum actuator displacement (obj_3), (c) Design 6 with maximum force transmission (obj_1), (d) and Design 7 as a balanced trade-off among all objectives.

we selected a design with a low torque variance and a short actuator displacement with a “not too low” force transmission).

Fig. 5 clearly shows that the solutions from SOOP (Design 1 and 2) are outside the Pareto set retrieved by the MOEAs; additionally, they are both non-dominated when compared to the rest of the set. Therefore, the true Pareto Front is actually larger than what was explored by the MOEAs. However, this does not mean that the MOEAs perform badly, but that the algorithms were attracted to specific regions of the objective space. This is clearly visible when observing the two-dimensional projections: Fig. 5(c) shows that most solutions are concentrated in what would be the Pareto Front if obj_1 was not considered (i.e., solutions that minimize both obj_2 and obj_3). In fact, Design 1 and 2 lie in the opposite regions, but are still non-dominated because of the additional third objective obj_1 . The opposite trend is visible also in the projection of Fig. 5(b): most of the solutions are not concentrated on what would be the Pareto Front if obj_3 was not considered (i.e., solutions that minimize both obj_1 and obj_2 , whereas obj_1 was supposed to be maximized), indicating that overall obj_3 has a bigger impact than obj_1 on the objective space exploration. From this figure, we can clearly observe that Design 1 lies on what would be the Pareto Front if obj_3 was not considered, whereas Design 2 lies on what would be the Pareto Front if also the constraint on the actuator con_7 is considered. From these observations, we can conclude that when considering force transmission only, Design 1 and 2 are overall the best solutions, indicating that BBBC for SOOP is a valid EA for robotic design optimization.

When comparing Design 3 to Design 1 (both $L_x > 50$), Design 3 renders lower forces, but it features smaller torque variance and a smaller actuator (therefore, the solutions do not dominate each other); however, the gain in the last objectives is

so small that it might not justify the gain in the first objective. Design 4 (also $L_x > 50$) has notably better torque variance than Design 1 and 3, as expected, but a lower force transmission. As shown by Fig. 5(d), achieving a more balanced torque spread on the finger joints requires longer actuators – and, therefore, lower force transmission.

Among the designs with $L_x \leq 50$, depicted in Fig. 7, Design 5 is the one with the lowest actuator displacement. However, since we observed an inversely proportional relationship between force and actuator (see Fig. 5(c)), Design 5 features the lowest force transmission among all possible solutions; additionally, its torque variance is high, resulting in unbalanced forces on the finger joints – which are still in a safe range for the user. For Design 6, we picked a trade-off solution considering force transmission and actuator displacement with no particular attention to the torque variance: specifically, we chose the solution with the maximum force transmission having $L_x \leq 50$. This design resulted in very similar values of force transmission and actuator displacements to Design 2 from SOOP; however, it has a lower torque variance – which is, surprisingly, the objective we did not consider while picking Design 4. This shows how MOOP provided a more optimized solution than SOOP, provided that designers are not interested in force transmission only. Finally, we picked Design 7 as a generic trade-off solution considering all the objectives, which produces lower forces than other designs but provides better torque balance and smaller actuators.

All solutions in Fig. 5 are equally suitable depending on the designer’s preference and, more specifically, based on the type of applications and use cases. U-HEX was previously proposed to be used not only for physical rehabilitation exercises but also for haptic or assistive uses. For haptic use, achieving smaller and lighter designs (therefore smaller actuator dis-

placements) should be a higher priority than torque variance or force transmission (i.e., Design 5). For physical rehabilitation, achieving maximum force transmission should be a higher priority than torque variance or actuator displacements to overcome high levels of spasticity of their fingers among the feasible solutions (i.e., Design 6). Finally, for assistive use, all objectives need to be optimized simultaneously: high-force transmission is needed to help users grasp objects at any weight in a stable manner, and low torque variance is needed to improve their safety while grasping objects of any shape or size, and low actuator displacement is needed to improve the portability (i.e., Design 7). Compared to Design 2 in SOOP, which offers a very similar solution to Design 6, the solutions in MOOP offer designers the luxury to select an *optimal* solution in parallel to their design needs.

The physical robot shown in Fig. 1 (first page) is Design 6.

VI. CONCLUSIONS

In this work, we presented a complete study on the optimization of U-HEX, an underactuated hand exoskeleton with a complex kinematic structure. We implemented two optimization design processes to find the correct link lengths to manufacture an optimal device. In the first process, we *only* focused on maximizing the force transmission while ensuring the device's safe and feasible operation through mechanical constraints, extending what we presented in our previous work [20]. In the second process, we converted some of the mechanical constraints into objectives: minimize torque variance and the desired actuator displacement. We implemented different optimization methods with various conditions (e.g., number of link lengths, optimization algorithm, survival strategy) to point out the best implementation of the optimization method for future designers. While combining different multi-optimization survival strategies, we implemented two new MOEAs, namely NS-BBBC and SP-BBBC, which performed competitively with respect to two of the most famous MOEAs in the state-of-the-art, NSGA-II [33] and SPEA2 [34]. The code is publicly available on MathWorks File Exchange².

In terms of robotic designs, our results indicate the potential benefits of different optimization problem settings depending on the requirements. For example, MOOPs allow the designer to choose a solution among alternatives with no change in the problem. Instead of choosing one objective as the selection criteria with no particular attention on the others (Design 3, 4, 5) or with an additional constraint to allow for the feasibility of the solution (Design 6), designers might opt for a solution with some compromise from multiple objectives simultaneously (Design 7). It is interesting to observe that implementing a SOOP and MOOP with the same additional constraint (con_7) resulted in somewhat similar solutions, therefore the designer should make their selection among MOOP and SOOP considering the trade-off between flexibility of chosen design and computational burden.

In terms of algorithms, our study found no statistical difference in optimality between GA and BBBC in MOOP,

although SPEA2 had the highest performance based on the hypervolume indicator. However, GA showed significant changes under varying conditions, unlike BBBC. Thus, GA is more suitable for designers needing diverse conditions, while BBBC provides more consistent results for those less familiar with optimization methods.

In the future, this study can be extended by using another survival strategy for MOOPs: "rank partitioning", which was developed to optimize the design of soft growing robots [39]. This method retrieves a single optimal solution rather than a Pareto set once the designer has established priorities among objectives – with no need for numerical values for each priority. Since the order of the objectives can produce a different design for specific applications, this method can quickly determine the targeted settings. Besides exploring different optimization methods, we will also examine the effects of the proposed improvements during real human-robot interaction by testing the physical exoskeletons. This investigation will include a thorough analysis of user experience and interaction forces to understand the practical impact and effectiveness of each design in enhancing human-robot collaboration.

ACKNOWLEDGEMENTS

The authors would like to thank Mazhar Eid Zyada for drawing the CAD models, and Ayse Yalcin and Ayodele Oyejide for printing and assembling the physical device.

REFERENCES

- [1] T. Poliero, M. Lazzaroni, S. Toxiri, C. Di Natali, D. G. Caldwell, and J. Ortiz, "Applicability of an active back-support exoskeleton to carrying activities," *Frontiers in Robotics and AI*, vol. 7, p. 579963, 2020.
- [2] A. Mauri, J. Lettori, G. Fusi, D. Fausti, M. Mor, F. Braghin, G. Legnani, and L. Roveda, "Mechanical and control design of an industrial exoskeleton for advanced human empowering in heavy parts manipulation tasks," *Robotics*, vol. 8, no. 3, p. 65, 2019.
- [3] T. Bützer, O. Lambercy, J. Arata, and R. Gassert, "Fully wearable actuated soft exoskeleton for grasping assistance in everyday activities," *Soft robotics*, vol. 8, no. 2, pp. 128–143, 2021.
- [4] F. Stroppa, C. Loconsole, S. Marcheschi, and A. Frisoli, "A robot-assisted neuro-rehabilitation system for post-stroke patients' motor skill evaluation with alex exoskeleton," in *Proceedings of the International Conference on NeuroRehabilitation (ICNR)*, 2017, pp. 501–505.
- [5] S. W. Brose, D. J. Weber, B. A. Salatin, G. G. Grindler, H. Wang, J. J. Vazquez, and R. A. Cooper, "The role of assistive robotics in the lives of persons with disability," *American Journal of Physical Medicine & Rehabilitation*, vol. 89, no. 6, pp. 509–521, 2010.
- [6] J. L. Pons, "Rehabilitation exoskeletal robotics," *IEEE Engineering in Medicine and Biology Magazine*, vol. 29, no. 3, pp. 57–63, 2010.
- [7] M. Sarac, M. Solazzi, and A. Frisoli, "Design requirements of generic hand exoskeletons and survey of hand exoskeletons for rehabilitation, assistive, or haptic use," *IEEE Transactions on Haptics (ToH)*, vol. 12, no. 4, pp. 400–413, 2019.
- [8] J. Van der Vorm, L. O'Sullivan, R. Nugent, and M. de Looze, "Considerations for developing safety standards for industrial exoskeletons," *Robo-Mate*, pp. 1–13, 2015.
- [9] C. Fisahn, M. Aach, O. Jansen, M. Moisi, A. Mayadev, K. T. Pagarigan, J. R. Dettori, and T. A. Schildhauer, "The effectiveness and safety of exoskeletons as assistive and rehabilitation devices in the treatment of neurologic gait disorders in patients with spinal cord injury: A systematic review," *Global spine journal*, vol. 6, no. 8, pp. 822–841, 2016.
- [10] R. Sioshansi and A. J. Conejo, *Optimization in Engineering*. Cham: Springer International Publishing, 2017, vol. 120.
- [11] R. B. Statnikov and J. B. Matusov, *Multicriteria Optimization and Engineering*. Springer Science and Business Media, 2012.
- [12] J. Andersson, "A survey of multiobjective optimization in engineering design," *Department of Mechanical Engineering, Linköping University, Sweden*, 2000.

²<https://www.mathworks.com/matlabcentral/fileexchange/167296>

- [13] J.-F. Bonnans, J. C. Gilbert, C. Lemaréchal, and C. A. Sagastizábal, *Numerical Optimization: Theoretical and Practical Aspects*. Springer Science and Business Media, 2006.
- [14] F. Stroppa, A. Soylemez, H. T. Yuksel, B. Akbas, and M. Sarac, "Optimizing exoskeleton design with evolutionary computation: An intensive survey," *Robotics*, vol. 12, no. 4, p. 106, 2023.
- [15] H. Norde, F. Patrone, and S. Tijs, "Characterizing properties of approximate solutions for optimization problems," *Mathematical Social Sciences*, vol. 40, no. 3, pp. 297–311, 2000.
- [16] B. Dizangian and M. Ghasemi, "Reliability-based design optimization of complex functions using self-adaptive particle swarm optimization method," *International Journal of Optimization in Civil Engineering*, vol. 5, no. 2, pp. 151–165, 2015.
- [17] Y. Nomaguchi, K. Kawakami, K. Fujita, Y. Kishita, K. Hara, and M. Uwasu, "Robust design of system of systems using uncertainty assessment based on lattice point approach: Case study of distributed generation system design in a Japanese dormitory town," *International Journal of Automation Technology*, vol. 10, no. 5, pp. 678–689, 2016.
- [18] D. Dumitrescu, B. Lazzarini, L. C. Jain, and A. Dumitrescu, *Evolutionary Computation*. CRC press, 2000.
- [19] M. Sarac, M. Solazzi, E. Sotgiu, M. Bergamasco, and A. Frisoli, "Design and kinematic optimization of a novel underactuated robotic hand exoskeleton," *Meccanica*, vol. 52, pp. 749–761, 2017.
- [20] B. Akbas, H. T. Yuksel, A. Soylemez, M. E. Zyada, M. Sarac, and F. Stroppa, "The impact of evolutionary computation on robotic design: A case study with an underactuated hand exoskeleton," in *IEEE International Conference on Robotics and Automation (ICRA)*, 2024.
- [21] D. E. Goldberg, J. Richardson *et al.*, "Genetic algorithms with sharing for multimodal function optimization," in *Genetic Algorithms and Their Applications: Proceedings of the Second International Conference on Genetic Algorithms*, vol. 4149, 1987.
- [22] D. E. Goldberg *et al.*, *Real-coded genetic algorithms, virtual alphabets and blocking*. Citeseer, 1990.
- [23] O. K. Erol and I. Eksin, "A new optimization method: Big Bang–Big Crunch," *Advances in Engineering Software*, vol. 37, no. 2, pp. 106–111, 2006.
- [24] A. Calanca, S. Toxiri, D. Costanzi, E. Sartori, R. Vicario, T. Poliero, C. Di Natali, D. G. Caldwell, P. Fiorini, and J. Ortiz, "Actuation selection for assistive exoskeletons: Matching capabilities to task requirements," *IEEE Transactions on Neural Systems and Rehabilitation Engineering*, vol. 28, no. 9, pp. 2053–2062, 2020.
- [25] D. E. Goldberg, *Genetic Algorithms in Search, Optimization, and Machine Learning*. Addison-Wesley, 1989.
- [26] D. E. Goldberg and K. Deb, "A comparative analysis of selection schemes used in genetic algorithms," in *Foundations of genetic algorithms*. Elsevier, 1991, vol. 1, pp. 69–93.
- [27] L. J. Eshelman and J. D. Schaffer, "Real-coded genetic algorithms and interval-schemata," in *Foundations of genetic algorithms*. Elsevier, 1993, vol. 2, pp. 187–202.
- [28] K. Deb, M. Goyal *et al.*, "A combined genetic adaptive search (genes) for engineering design," *Computer Science and Informatics*, vol. 26, pp. 30–45, 1996.
- [29] H.-G. Beyer and H.-P. Schwefel, "Evolution strategies – a comprehensive introduction," *Natural computing*, vol. 1, pp. 3–52, 2002.
- [30] H. M. Genç, I. Eksin, and O. K. Erol, "Big bang-big crunch optimization algorithm hybridized with local directional moves and application to target motion analysis problem," in *IEEE International Conference on Systems, Man and Cybernetics*, 2010, pp. 881–887.
- [31] C. A. C. Coello, "Theoretical and numerical constraint-handling techniques used with evolutionary algorithms: A survey of the state of the art," *Computer Methods in Applied Mechanics and Engineering*, vol. 191, no. 11–12, pp. 1245–1287, 2002.
- [32] K. Deb, *Multi-objective Optimization using Evolutionary Algorithms*. John Wiley and Sons, Ltd, 2001.
- [33] K. Deb, A. Pratap, S. Agarwal, and T. Meyarivan, "A fast and elitist multiobjective genetic algorithm: NSGA-II," *IEEE Transactions on Evolutionary Computation*, vol. 6, no. 2, pp. 182–197, 2002.
- [34] E. Zitzler, M. Laumanns, and L. Thiele, "SPEA2: Improving the strength pareto evolutionary algorithm," *TIK-report*, vol. 103, 2001.
- [35] K. Shang, H. Ishibuchi, L. He, and L. M. Pang, "A survey on the hypervolume indicator in evolutionary multiobjective optimization," *IEEE Transactions on Evolutionary Computation*, vol. 25, no. 1, pp. 1–20, 2020.
- [36] C. M. Fonseca, L. Paquete, and M. López-Ibáñez, "An improved dimension-sweep algorithm for the hypervolume indicator," in *IEEE International Conference on Evolutionary Computation*, 2006, pp. 1157–1163.
- [37] L. While, P. Hingston, L. Barone, and S. Huband, "A faster algorithm for calculating hypervolume," *IEEE Transactions on Evolutionary Computation*, vol. 10, no. 1, pp. 29–38, 2006.
- [38] R. A. King, K. Deb, and H. Rughooputh, "Comparison of NSGA-II and SPEA2 on the multiobjective environmental/economic dispatch problem," *University of Mauritius Research Journal*, vol. 16, no. 1, pp. 485–511, 2010.
- [39] F. Stroppa, "Design optimizer for planar soft-growing robot manipulators," *Elsevier Engineering Applications of Artificial Intelligence*, vol. 130, p. 107693, 2024.

Baris Akbas is a graduate student in the Department of Computer Engineering at İstanbul Technical University. He received his B.S. degree in Computer Engineering at Kadir Has University in 2024. He worked as a teaching assistant and a research assistant in EVO Lab from 2023 to 2024. His research interests include optimization, robotics, and artificial intelligence.

Huseyin Taner Yuksel received his B.S. degree in Computer Engineering at Kadir Has University, İstanbul, in 2024. He worked as a research assistant as a member of EVO Lab between 2023–2024. He was a board member of the Engineering Club, Kadir Has University, İstanbul, until 2023. His research interests include optimization and robotics.

Aleyna Soylemez received her B.S. degree in Computer Engineering at Kadir Has University, İstanbul, in 2024. She worked as a teaching assistant and research assistant as a member of EVO Lab between 2023–2024. She was a board member of the Engineering Club, Kadir Has University, İstanbul, until 2023. Her research interests include search and optimization, and robotics.

Mine Sarac is an Assistant Professor in the Department of Mechatronics Engineering at Kadir Has University, İstanbul, Türkiye, specializing in the fields of Human-Machine Interaction and Haptics. She received her B.S. degree from Yeditepe University, İstanbul, in 2011, an M.S. degree from Sabanci University, İstanbul, in 2013, and a PhD degree from Scuola Superiore Sant'Anna in 2018. She received postdoc training at CHARM Lab, Stanford University, California, USA, until 2021. Her research interests include haptics, robotics, virtual environments and simulation, and rehabilitation. She is an IEEE member.

Fabio Stroppa (Eng., Ph.D.) is an Assistant Professor in the Department of Computer Engineering at Kadir Has University, İstanbul, Türkiye, specializing in the fields of Artificial Intelligence and Human-Machine Interaction. He received his B.S. and M.S. degrees in Computer Science Engineering from the Polytechnic University of Bari, Italy, in 2011 and 2013, respectively, and the Ph.D. in Perceptual Robotics from Scuola Superiore Sant'Anna, Pisa, Italy, in 2018. He received postdoc training at CHARM Lab, Stanford University, California, USA, from 2019 to 2021. He is currently the head of EVO Lab. His publications and main research interests include search and optimization, evolutionary computation, robotics, haptics, motion planning, shared control, computer vision, robotic-based neurorehabilitation, and bioinformatics.